Accepted Article

Supplementary Information:

The receptor tyrosine kinase EphB2 promotes hepatic fibrosis in mice

Patrice N. Mimche[1], Lauren M. Brady[1], Christian F. Bray[1], Sylvie M. Mimche[2], Manoj Thapa[3], Thayer P. King[1], Kendra Quicke[1], Courtney D. McDermott[1], Choon M. Lee[2], Arash Grakoui[3], Edward T. Morgan[2] and Tracey J. Lamb[1]

[1]Division of Infectious Diseases, Department of Pediatrics, Emory University School of Medicine and Emory Children's Centre, 2015 Uppergate Drive, Atlanta, Georgia 30322, USA.

[2] Department of Pharmacology, Emory University School of Medicine, Atlanta, GA 30322

[3]Division of Microbiology and Immunology, Emory Vaccine Center, Emory University School of Medicine, Atlanta, GA 30322

This article is protected by copyright. All rights reserved.

Accepted Article

Materials and Methods

Rodent malaria infection. Female C57BL/6 wild type (WT) mice aged 6-12 weeks were bred in-house or purchased from The Jackson laboratory (Bar Harbor, ME, USA). *EphB2-/-* mice on a C57BL/6 background were re-derived and bred in-house under a heterozygous breeding system. Mice were given water and food (LabDiet, MO, USA: chow 5001) *ad libitum* and housed under standard conditions. Infections were initiated intraperitoneally with $1x10^6$ *Pb*A iRBCs (clone15cy1) or $1x10^5$ *Pcc*AS iRBCs obtained from donor mice. Parasitemia was monitored by counting 300-500 RBC of Giemsa-stained blood smears and in tissues by quantitative PCR. All experiments were approved and carried out according to protocols approved by the Institutional Animal Care University Committee at Emory University.

CCL_4 model of hepatic fibrosis. Mice aged 6-12 weeks were injected intraperitoneally with 2µl/g of CCL_4 (Sigma) (adjusted at 10% concentration in olive oil) or olive oil three times per week for 4 weeks. Mice were sacrificed by CO_2 inhalation 72 hours after the last dose of CCL_4 and the livers removed and processed for further analysis.

Assessment of liver injury

Mice were sacrificed by CO_2 inhalation and blood samples collected into 20µl of heparin and centrifuged for collection of plasma within 1 hour of blood collection and frozen at -80^{o}C until analysis. Plasma samples from naive and infected mice were processed in a

This article is protected by copyright. All rights reserved.

single batch for determination of serum alanine aminotransferase (ALT) and aspartate aminotransferase (AST) levels using a DC Element chemistry analyser (HESKA).

Depletion of Kupffer cells and neutrophils/monocytes. Kupffer cells were depleted by intravenous injection of 200µl of clodronate-loaded liposomes or empty liposome-PBS in control mice on day -1 of malaria infection (ClodronateLiposomes.org, Amsterdam, Netherlands). Ly6G-expressing neutrophils and Ly6C-expressing inflammatory monocytes were depleted by injecting mice with 2x 300 µg intraperitoneal doses of anti-Gr-1 monoclonal antibody (clone RB6-8C5) or a Rat IgG isotype control antibody (clone RTK2071) (Biolegend) on days -1 pre-infection and day 1 post-infection.

Assessment of liver fibrosis. Livers were removed from euthanized mice, embedded in OCT compound and immediately snap-frozen in liquid nitrogen. Sections 5µm thick were stained with hematoxylin-eosin to visualize infiltration of leukocytes or picrosirius red (Sigma Aldrich) to visualize hepatic collagen deposition. Imaging was performed on a widefield Zeiss Axioplan 2 microscope in at least 10 low-power non-overlapping random fields (magnification 20x) per mouse using a polarized light filter and quantified using ImageJ software (NIH, Bethesda, MD).

Immunohistochemistry. Sections of cryopreserved liver 5µm thick were stained with the following antibodies: anti- α-SMA-Cy3^{TM} clone 1A4 dilution 1:500 (Sigma), anti-mouse EphB2 (clone 512001 or clone 512013 at 2µg/ml (R&D systems) and NIMP-14

This article is protected by copyright. All rights reserved.

Accepted Article

clone ab2557 at dilution 1:200 (Abcam) using standard methodology. Sections were then stained with secondary rat or rabbit antibodies labelled with NorthernLights 493® or NorthernLights 577® (R&D Systems) and nuclei counterstained with mounting medium containing DAPI (VectorShield). Images were captured using a Carl Zeiss confocal microscope and analyzed using Image J software.

RNA extraction and cDNA synthesis. Cells or tissue were homogenized in RNA Stat60® and total RNA extracted using standard phenol-chloroform protocols followed by DNase treatment of RNA extracted using RNA-II purification kit (Nachery-Nagel). A total of 100ng of RNA per sample was converted into cDNA using Superscript II (Life Technologies) at 42°C for 50min, 70°C 15min, in the presence of 5uM oligo $(dT)_{16-18}$, 5mM Dithiothreitol (DTT), 0.5mM dNTPs (all Life Technologies), 8U RNAsin (Promega), 50mM Tris-HCl pH8.3, 75mM KCl and 3mM $MgCl_2$. The cDNA was treated with 2.5U RNAse H (Affymetrix) at 37°C for 20min to remove any remaining RNA residues.

Quantitative PCR. Real-time qPCR reactions were performed using Quantitect SYBR Green PCR reagent (Qiagen). PCR amplification was performed with 5µl cDNA sample (diluted 1:10), 2µM of each primer, 7µl of QPCR SYBR green mix and plates run using Applied BioSystems FAST 7000 Sequence detection system (ABI Prism FAST 7000). Primer sequences are shown in Supporting Table S1. Transcripts were normalized to two different housekeeping genes (Ubiquitin and β-actin) and expression levels calculated using the 2^{-DDCt} method. The fold change of transcription for individual

This article is protected by copyright. All rights reserved.

Accepted Article

infected animal was calculated in relation to the average expression in naïve mice for each group at each time point.

Tissue processing for flow cytometry. Livers and brains were pressed through a 40mm cell strainer, suspended in Iscove's Modified Dulbecco's Medium (IMDM) containing 100units / ml penicillin, 100µg / ml streptomycin, 1µM of L-glutamine, 12mM HEPES, 0.5mM sodium pyruvate, 5 X 10^{-5}M mercaptoethanol (all Gibco) and 10% heat inactivated fetal calf serum (FCS) (PAA Laboratories) containing Liberase-TL synthetic collagenase (Roche) at a final concentration of 0.3mg/ml and dispase (Invitrogen) at final concentration 2mg/ml and further incubated for 45 min at 37^{o}C. The suspension was overlaid on a 30% Percoll gradient and centrifuged at 1800*g* for 10min. The pellet was collected and supernatant discarded. Red blood cells (RBC) were removed from aseptic single cell suspensions of splenocytes or liver and brain single cell suspensions by incubation in an NH_4Cl-based RBC lyzing solution (eBioscience).

For flow cytometry samples were incubated with Fc blocking antibodies (CD16/CD32 clone 2.4G2) and then with various antibody cocktails mixtures containing: CD3 (APC-Cy7, clone 17A2), CD4 (Pacific Blue, clone GK1.5), CD8 (FITC, clone 53-6.7), Ly6C (PE, clone HK1.4), Ly6G (FITC, clone 1A8), CD11c (APC, clone N418), CD11b (eFluor450, clone M1/70), and F4/80 (PE-Cy7, clone BM8) (Biolegend). Intracellular cytokine staining on splenic T cells was undertaken after incubation for 6 hours on immobilized anti-CD3 (50µl / well at 5µg / ml) (clone 17A2) and soluble CD28 (2µg / ml) (clone 37.51) (eBioscience) in the presence of 10µg / ml brefeldin A (Sigma). After surface staining, cells were fixed with 2% paraformaldehyde, permeabilized with 0.05%

This article is protected by copyright. All rights reserved.

Accepted Article

saponin (Sigma) and stained with anti-IFN-γ-PE (clone XMG1.2). Flow cytometric acquisition was performed on a FACS Canto (BD Biosciences) and data analyzed using FlowJo software (TreeStar).

For detection of EphB receptor surface expression, liver nonparenchymal cells were sequentially stained with recombinant chimeric mouse Fc-EphrinB2 protein (2µg/ml) (R and D) followed by a biotinylated goat anti-human IgG Fcγ (eBioscience) and then Streptavidin-APC (Biolegend). HSCs were identified as UV autofluorescence-positive and α-SMA was detected as described previously[1] using PE-αSMA labelled antibody clone 1A4 (R&D Systems).

Splenocytes FACS cell sorting. For FACS sorting of splenic populations, B cells were first removed using CD19+ positive selection beads (Miltenyi Biotech) and all populations were sorted from CD19 negative splenocytes. Antibodies used were CD4+T cells (CD3+CD4+), CD11c+ dendritic cells (DCs) (CD11c+), CD8+T cells (CD11c- CD8+CD3+) and CD11b+ (CD11c- CD8- CD11b+) were sorted on a FACS Aria II (BD biosciences) before being stored in RNA Stat60 at -80^{o}C until processed for RT-qPCR.

Hepatocyte isolation and stimulation assay. Mouse hepatocytes were isolated by a two-step *in situ* collagenase perfusion procedure as described by Kinloch *et al*[2]. Livers of naïve mice were perfused *in situ* with Krebs-Ringer bicarbonate buffer followed by 0.3mg/ml type IV collagenase (Sigma, MO). Hepatocyte preparations were plated in a 24-well collagen-coated plate at a density of 1x10^{6} cells/well in Williams E medium containing 10mM HEPES pH 7.4, 150nM insulin, 50nM dexamethasone, 100units / ml

This article is protected by copyright. All rights reserved.

penicillin, 100µg / ml streptomycin and 10% heat inactivated FCS (CWE). 4h later, cells were overlaid with fresh serum-free CWE medium containing Matrigel (0.23mg / ml, BD Biosciences). 24 hours later hepatocytes were cultured in serum sufficient CWE medium with intact mature *Pb*A schizonts, prepared according to standard procedures, at a concentration of $50x10^6$cells in 50µl. Lysed preparations were made by snap freezing and thawing 3 times. Naïve red blood cells (nRBCs) were obtained from naïve animals and naïve RBC lysates were made in an identical fashion to iRBC lysates. Some wells were incubated with LPS from *Salmonella minnesota* (Alexis) (1µg/ml) and recombinant mouse tumor necrosis factor-α (rTNFα) (10ng/ml).

Western blot. Liver lysates and hepatocytes were prepared with RIPA buffer containing 1x EDTA/proteinase-phosphatase inhibitor cocktail (Pierce). The lysate supernatant was stored at -80^{o}C until used for immunoblotting. Protein extracts were separated by SDS-PAGE electrophoresis and blotted onto nitrocellulose membrane. Blots were incubated overnight with the following primary detection antibodies: anti-mouse TNF-α clone D2D4 (Cell signalling technology) NFκBp65 clone 27F9.G4 dilution 1:1000 (Rockland^{TM}); anti-mouse IKKβ clone 42D1 at dilution 1:500 (Pierce), phosphoNFκBp65 clone 93H1 dilution 1:1000 and phosphoIKKαβ clone 16A6 (Cell signalling technology) and anti-mouse β-actin clone AC-15 at dilution 1:1000 (Pierce). Blots were then stained for 1 hour with rat or rabbit HRP-conjugated secondary antibodies used at a dilution 1:2000 (R and D Systems). Finally, blots were developed using ECL substrate per the manufacturer's instructions (Pierce) and quantified using densitometry measurements on Image J software.

This article is protected by copyright. All rights reserved.

Accepted Article

Statistical analysis. Differences between groups of animals were assessed using the non-parametric Mann Whitney-U test or parametric Student's t-test or General Linear Modelling (GLM), a variant of analysis of variance (ANOVA) including all 1st order interactions in Minitab software (Minitab, Inc.). Data or residual variation was assessed for normality using Anderson-Darling test and heterogeneity of variance using the F-test or Bartlett's test. Data that did not meet these requirements for parametric testing was logarithmically or square root transformed. For ANOVA, F values quoted are from the minimal model of the data with all insignificant terms removed. Values of $p<0.05$ were considered statistically significant.

Supplementary references

1. Dunham RM, Thapa M, Velazquez VM, Elrod EJ, Denning TL, Pulendran B*, et al.* Hepatic stellate cells preferentially induce Foxp3+ regulatory T cells by production of retinoic acid. *Journal of immunology* 2013, **190**(5)**:** 2009-2016.

2. Kinloch RD, Lee C-M, van Rooijen N, Morgan ET. Selective role for tumor necrosis factor-α, but not interleukin-1 or Kupffer cells, in down-regulation of CYP3A11 and CYP3A25 in livers of mice infected with a noninvasive intestinal pathogen. *Biochemical Pharmacology* 2011, **82**(3)**:** 312-321.

This article is protected by copyright. All rights reserved.

Accepted Article

Supplemental Figures Legends:

Figure S1: *Ephrin B1/B2* mRNA levels are not altered while EphB2 proteins increase in rodent malaria infection. (**A**-**B**) C57BL/6 mice were infected with 10^6 Pb*A* iRBCs or 10^5 *Pcc* iRBCs (**C** and **D**) with four mice per group. As controls for infection, 2 mice were injected with Kreb's saline solution. *EphrinB1*, *EphrinB2* mRNA from brain, lung, spleen and liver samples measured by qPCR is shown at days 2 (white bars), 4 (black bars) and 6 (grey bars) post *Pb*A infection (**A**-**B**) or days 6 (white bars), 9 (black bars) and 12 (grey bars) post *Pcc*AS infection (**C**-**D**). RNA expression is quantified as fold change relative to the average transcripts measured in the naïve control mice at each time point. The bars represent the mean of data pooled from 2 identical experiments in total of n=8 mice. The error bars represent ±SEM from the cumulative data from both experiments. (**E**) Confocal microscopy images showing protein expression of EphB2 in the liver of naïve and *Pb*A and *Pcc*AS infected mice.

Figure S2: *EphB2-/-* mice have similar plasma levels of liver damages enzymes compared to infected littermates animals. C57BL/6 mice were infected with 10^6 *Pb*A iRBCs or 10^5 *Pcc*AS iRBCs with four mice per group. As controls for infection, 2 mice were injected with Kreb's saline solution. At day 6 post infection with *PbA* (**A**, **B**) or *Pcc*AS (**C**, **D**) levels of liver enzymes were measured in the plasma. Plasma levels of aspartate transaminase (AST) (**A**, **C**) or alanine aminotransferase (ALT) (**B** and **D**) were measured. The box plots represent the cumulative data from 2 identical experiments and in total n=8 and show the median, 25% and 75% with maximum / minimum

This article is protected by copyright. All rights reserved.

Figure S3: Reduced liver fibrosis in *EphB2-/-* mice injected with CCL_4. *EphB2-/-* (n=3) and littermate control (n=4) mice were repeatedly injected with CCL_4 as described in materials and methods. As negative controls, 2 mice per genotype were injected with olive oil. (**A**) Liver sections were stained with picrosirius-red and positive areas were quantified using image J software. (**B**) Liver sections were stained with α-SMA-Cy3™ antibody for 1 hour. Images were captured using a Carl Zeiss confocal microscope and analyzed using Image J software. MFI indicate mean fluorescence intensity of α-SMA-Cy3™ positive areas in 12 randomly selected non-overlapping images per mouse. (**C**) Messenger RNA levels of profibrotic markers *COL1a1*, *α-SMA*, *TGF-β1*, *PDGFRβ* were measured by qPCR (normalized to β-actin levels). ***p<0.05* Mann Whitney-U test.

Figure S4: Reduced transcription of inflammatory cytokines mRNA in the liver of CCL_4-treated *EphB2-/-* mice: *EphB2-/-* mice (n=3) and littermate control mice (n=4) were repeatedly injected with CCL_4 as described in materials and methods. As negative controls, 2 mice per genotype were injected with olive oil. Messenger RNA levels of pro-inflammatory cytokines TNF-*α, IL-6* and the immunoregulatory cytokine *IL-10* were measured by qPCR (normalized to β-actin levels). ***p<0.05;* ns not significant Mann Whitney-U test.

Figure S5: Immune cells infiltration is reduced in the liver of CCL_4-treated *EphB2-/-* mice. *EphB2-/-* mice (n=3) and littermate control mice (n=4) were repeatedly injected with CCL_4 as described in materials and methods. As negative controls, 2 mice per genotype were injected with olive oil. (**A**) Liver sections were stained with H&E and liver non-parenchymal cells suspension enumerated using a Neubauer counting chamber.

This article is protected by copyright. All rights reserved.

Accepted Article

(**B**) Flow cytometry analysis of F4/80+CD11b+ cells population in the liver of *EphB2+/+* and *EphB2-/-* mice treated with CCL_4. ***p<0.05** Mann Whitney-U test.

Figure S6: *EphB2-/-* mice have no apparent defect in splenic or brain T cell responses during *Pb*A infection. C57BL/6 mice were infected with 10^6 *Pb*A iRBCs with 5 mice per group. As controls for infection, 2 mice were injected with Kreb's saline solution. At day 6 post infection the numbers of leukocytes accumulating in the spleen (**A**) or brain (**B**) were enumerated and stained intracellularly for IFN-γ (**C**: spleen; **D**: brain). All graphs represent the median ± maximum / minimum.

Figure S7: Reduced infiltration of T cells in the liver of *EphB2-/-* mice infected with rodent malaria: *EphB2-/-* and littermate control mice were infected with 10^6 *Pb*A iRBCs with 5 mice per group. As controls for infection, 2 mice were injected with Kreb's saline solution. (**A**) CD4+ and CD8+ T cells enumerated in the liver of *EphB2-/-* and littermates controls mice infected with *Pb*A at day 6 post-infection. (**B**) CD4+ and CD8+ T cells enumerated in the liver of *EphB2-/-* and littermate control mice infected with *Pcc*AS at day 12 post-infection. (**C**) Messenger RNA level of the inflammatory cytokine *INF-γ* in *Pb*A-infected mice at day 6 post-infection and (**D**) *Pcc*AS-infected mice at day12 post-infection. ***p<0.05;** ns not significant; Mann Whitney-U test.

Figure S8: Livers of *EphB2-/-* CCL_4 treated mice have defective transcription of adhesion molecules and chemokines *EphB2-/-* mice (n=3) and littermate control mice (n=4) were repeatedly injected with CCL_4 as described in materials and methods. As

This article is protected by copyright. All rights reserved.

negative controls, 2 mice per genotype were injected with olive oil. Messenger RNA levels of adhesion molecules *ICAM1*, *VCAM1* and chemokines/chemokine receptors *CCR2*, *CXCL10*, *CCL2* were measured by qPCR (normalized to β-actin levels). ***p<0.05* Mann Whitney-U test.

Figure S9: Depletion of Kupffer cells/macrophages attenuates immune cell recruitment, α-SMA expression and pro-inflammatory cytokines/chemokines in the liver of *Pb*A-infected mice at day 6 post-infection: Macrophages/Kupffer cells were depleted from mice using clodronate-loaded liposomes the day before infection with 10^6 *Pb*A with 8 mice per group. As controls for liposome injection, mice were injected with PBS liposomes. As controls for infection, 2 mice each were injected clodronate-loaded or PBS liposomes and injected with Kreb's saline solution. (**A**) Liver sections were stained with primary and secondary antibodies for EphB2. (**B**) Representative photomicrographs of H&E-stained sections of the liver (magnification 20x). (**C**) Liver sections were stained overnight with α-SMA-Cy3™ antibody. Images were captured using a Carl Zeiss confocal microscope and analyzed using Image J software. MFI indicate mean fluorescence intensity of αSMA-Cy3™ positive areas in 12 randomly selected non-overlapping images per mouse. (**D**) Messenger RNA levels of *TNF-α*, *IL-10*, *VCAM1*, *CCR2*, and *CCL2* were measured by qPCR (normalized to β-actin levels). CLO= Clodronate ***p<0.05;* ns not significant; Mann Whitney-U test.

Figure S10: Schematic of events plausibly involved in EphB2-mediated liver fibrosis. (1) Upon blood stage malaria or CCL_4-induced liver injuries, hepatocytes

This article is protected by copyright. All rights reserved.

Accepted Article

become activated and inflamed. Hepatic NF-κB and inflammation are enhanced by the presence of EphB2. (2) This inflammationpromotes the recruitment of immune cells (T cells, EphB2+ monocyte/macrophage among others) to the site of injury increasing the pool of EphB2 expressing cells in the liver. (3) Liver resident EphB2+ macrophages (Kupffer cells) in addition to recruited EphB2+ monocyte/macrophage release profibrotic cytokines/ chemokines (4) critical for the transdifferentiation of quiescent hepatic stellate cells into myofibroblast-secreting extracellular matrix (5). Macrophage depletion drastically reduced liver EphB2 expression, secretion of pro-inflammatory cytokines/chemokines and ultimately attenuates liver fibrosis.

This article is protected by copyright. All rights reserved.

Table S1: Mouse primer sequences.

Gene	Forward Primer	Reverse Primer
ephrin B1	TCGCAAGCATACACAGCAGCGG	ATGATGATGTCGCTGGGCTCGG
ephrin B2	CAGAAGAACCCTGCTTGCCTGG	AGCAAGCAGCCTTGACCTGC
ephrin B3	AGACTTTGGGGGAGTTGGTGCC	CAGCCCCGCAAAACCTAACAGC
EphB1	TTACAGCACAGGCCGAGGGGAGTTCG	AACTGGCCCATGATGCTCGCC
EphB2	ACGCCACGGCCATAAAAAGCCC	TTGCCACTGTAGCGCCCATAGC
EphB3	ATTGGGCATCAAGCCACCCAGC	TGCTCTGTAACCGAGGTGTCGC
EphB4	TTGAGCCCTGGGTGGCAATCCG	AGGCACCTCACGGTCAGTGG
EphB6	ACTCTAAGCTGCGAGCAGACGC	GCCAGGCTTGCCTTCTTGTCTGG
P. berghei ANKA 18S	AAGCATTAAATAAAGCGAATACATCCTTAC	GGAGATTGGTTTTGACGTTTATGTG
P. chabaudi AS MSP1	ACAGTAACACAAGAAGGAAC	GATACTTGTGTTGATGCTGG
IFN- γ	AACGCTACACACTGCATCTTGG	GCCGTGGCAGTAACAGCC
TNF-a	TCTCATTCCTGCTTGTGGC	CACTTGGTGGTTTGCTACG
IL-6	ACACATGTTCTCTGGGAAATCGT	AAGTGCATCATCGTTGTTCATACA
Col1a1	GGAGAGTACTGGATCGACCCTAAC	ACACAGGTCTGACCTGTCTCCAT
IL-10	CAAGGCAGCCTTGCAGAAA	CTAAGAGCAGGCAGCATAGC
CCL2 (MCP-1)	GGCTCAGCCAGATGCAGTTAA	CCTACTCATTGGGATCATCTTGCT
MIP-2	ACCAACCACCAGGCTACA	TCĜAGGGTCAAGGCAAACT
TGF-β1	ATCGACATGGAGCTGGTGAAA	TGGCGAGCCTTAGTTTGGA
α-SMA	CGGGAGAAAATGACCCAGATT	AGGGACAGCACAGCCTGAATAG
iNOS	CTTCACGGGTCAGAGCCACAGTCC	GAGCCAAAGCCAAACACAGCATAC
CCR2	GAAGGAGGGAGCAGTGTGTACAT	CCCCCACATAGGGATCATGA
ICAM-1	CAGTCTGCACCCAGTGCTCGTG	ACGGGTTGAAGCCATTGC
VCAM-1	ATTATGCCGTCGCGAGGTT	TCAGTCCAAGCAACACTCTCTGA
P-SELECTIN	CGTCTCAGAAAGAAAGATGATGGAA	GCAGCGTTAGTGAAGACTCCGTAT
CXCL-10	GACGGTCCGCTGCAACTG	GCTTCCCTATGGCCCTCATT
PDGFRβ	CTCAGGGTTTTCCGCAATCA	TATCACCCCCTCCAGGAAGTC

Accepted Article

This article is protected by copyright. All rights reserved.

Figure S1

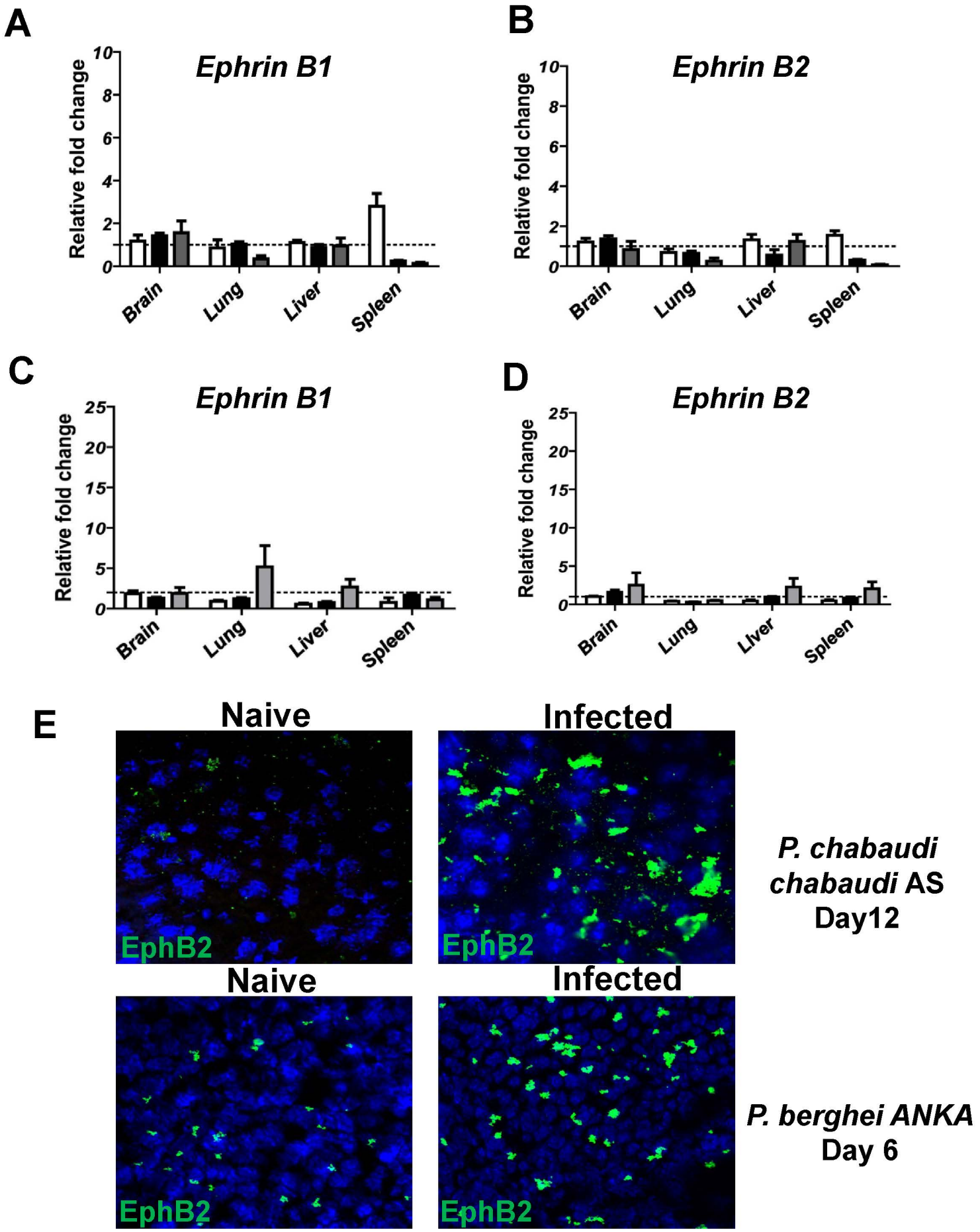

This article is protected by copyright. All rights reserved.

Figure S2

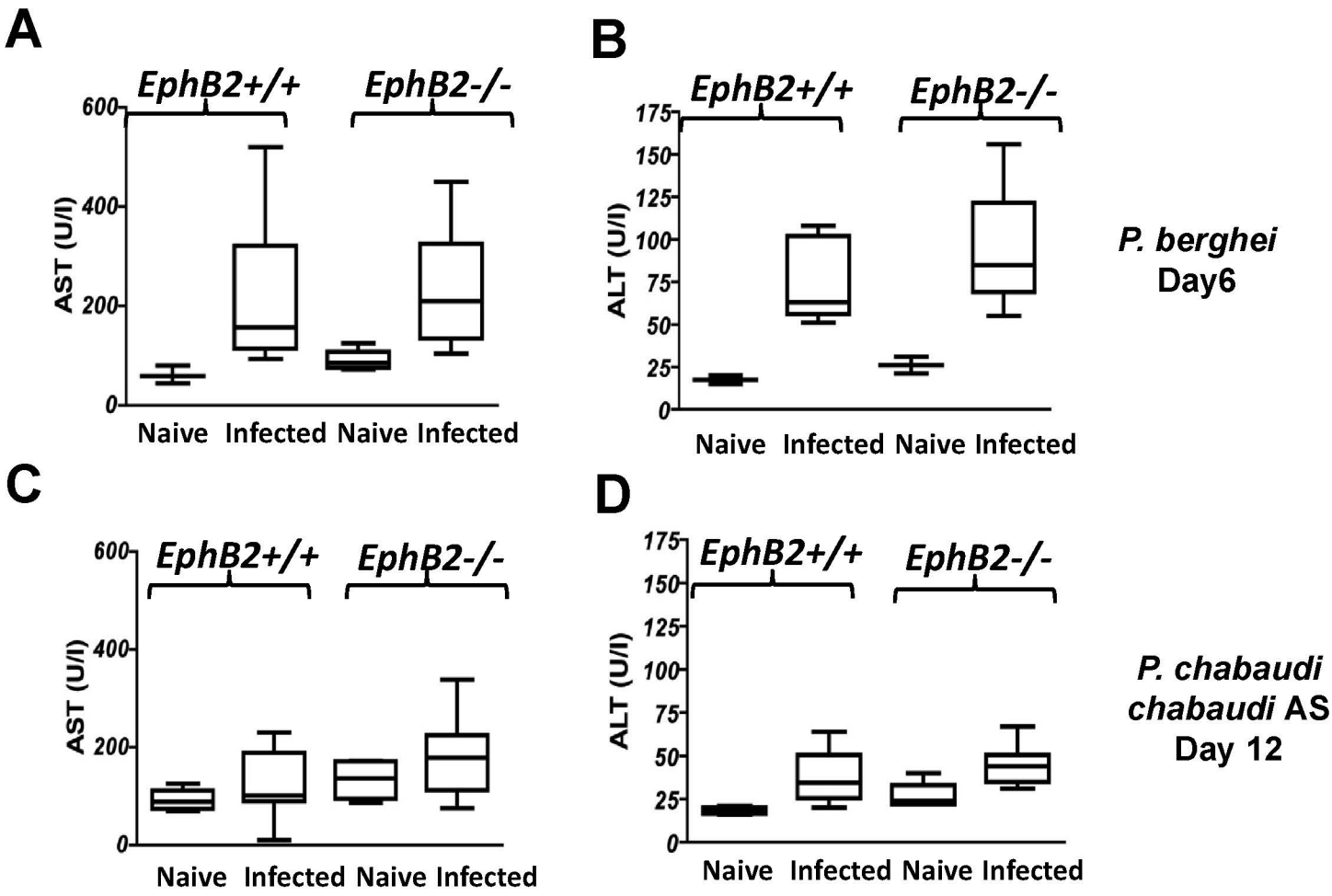

This article is protected by copyright. All rights reserved.

Figure S3

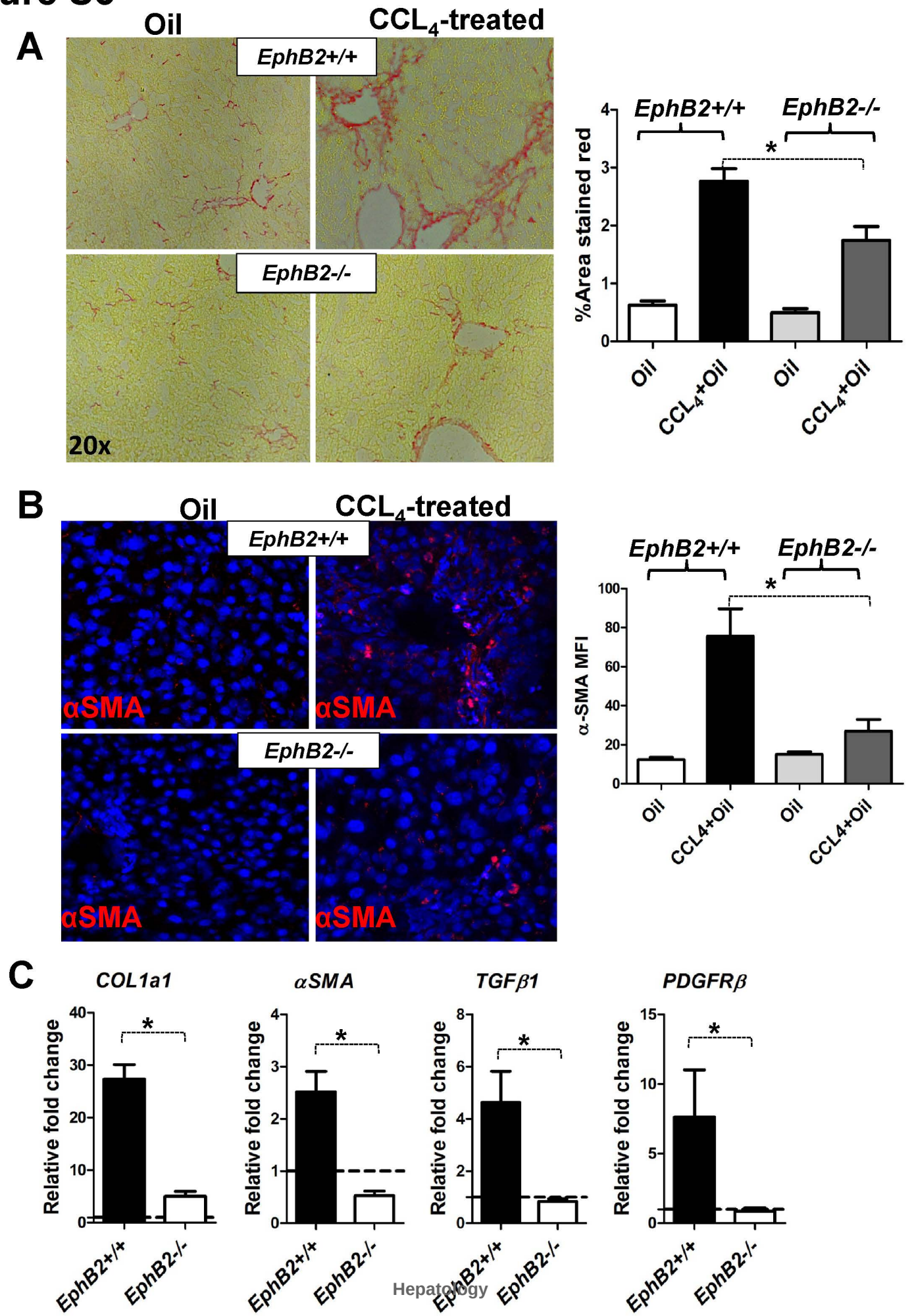

This article is protected by copyright. All rights reserved.

Figure S4

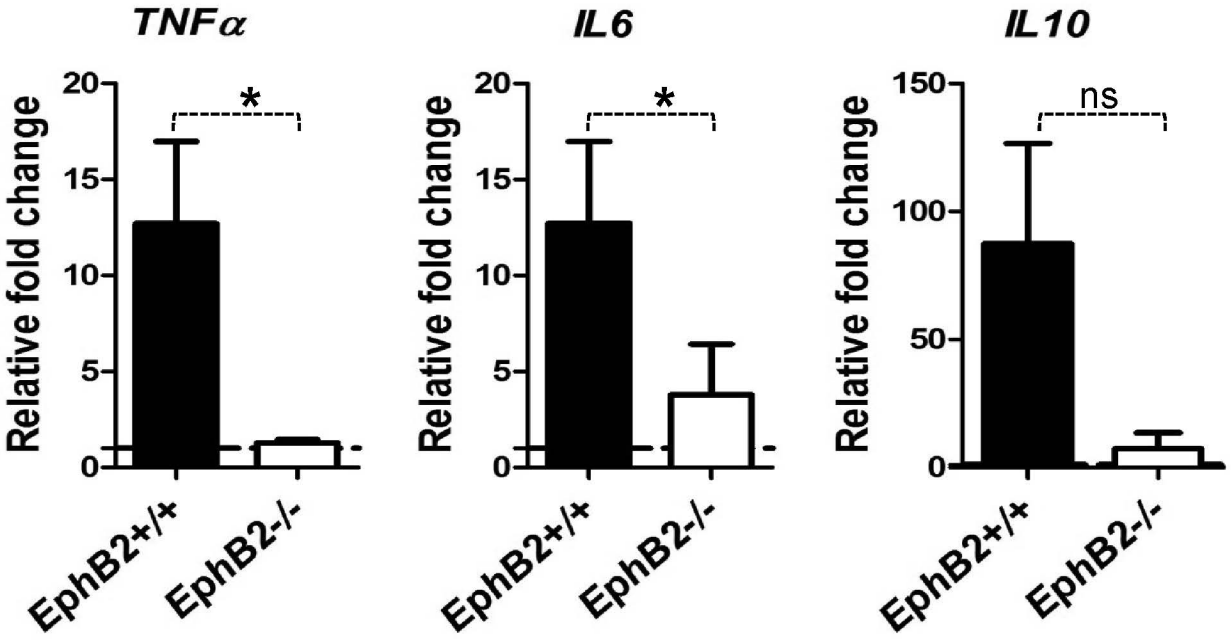

This article is protected by copyright. All rights reserved.

Figure S5

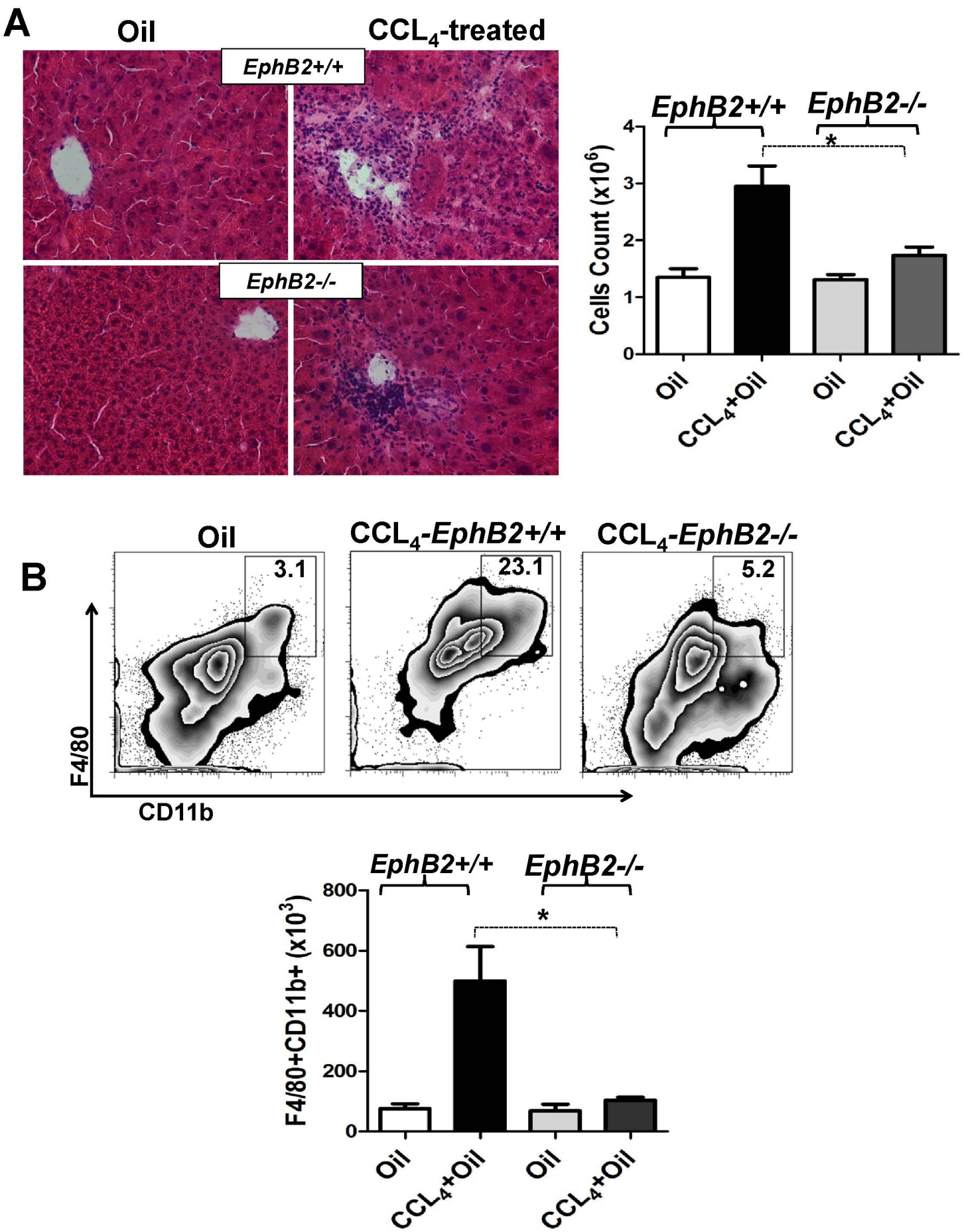

This article is protected by copyright. All rights reserved.

Figure S6:

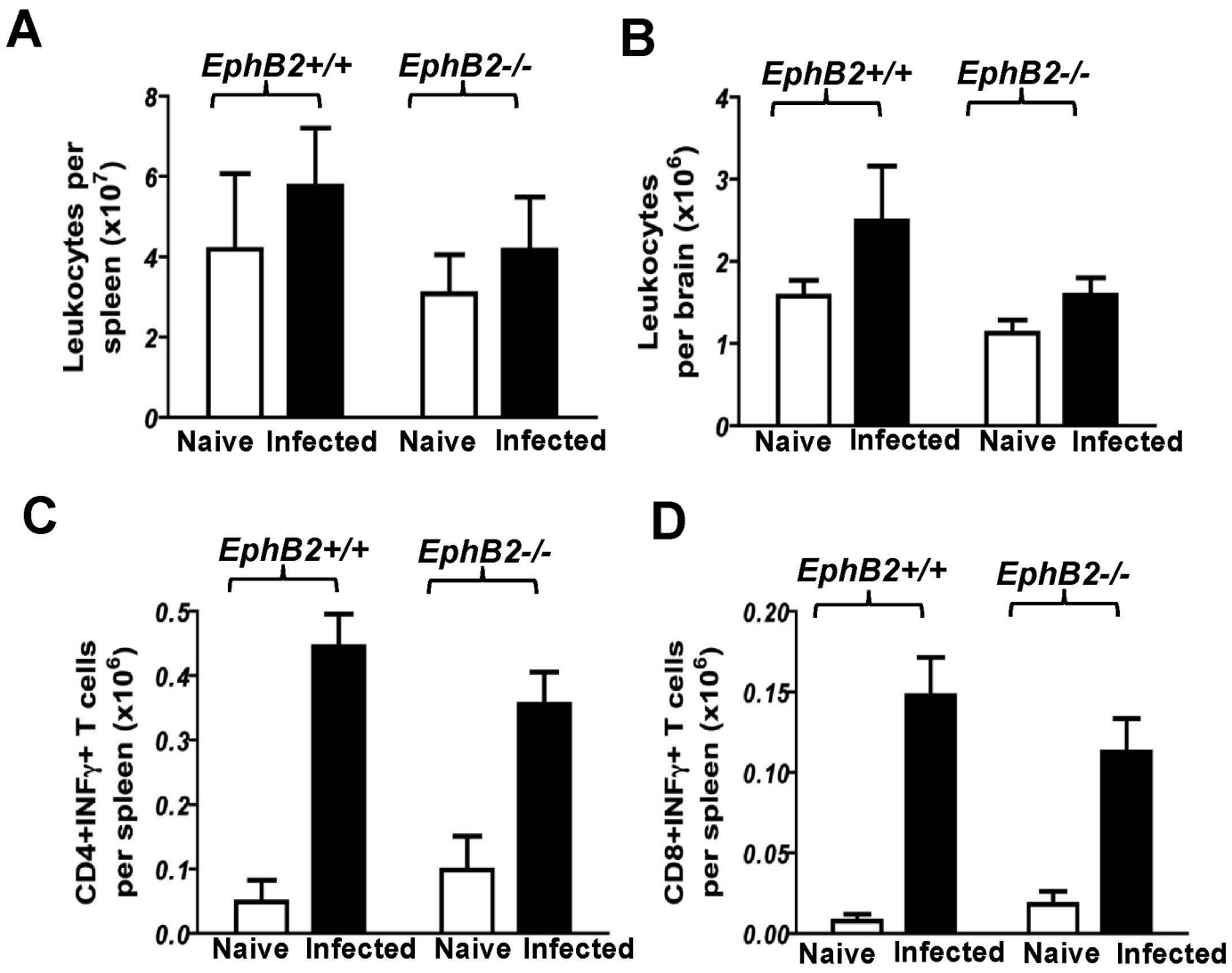

This article is protected by copyright. All rights reserved.

Figure S7

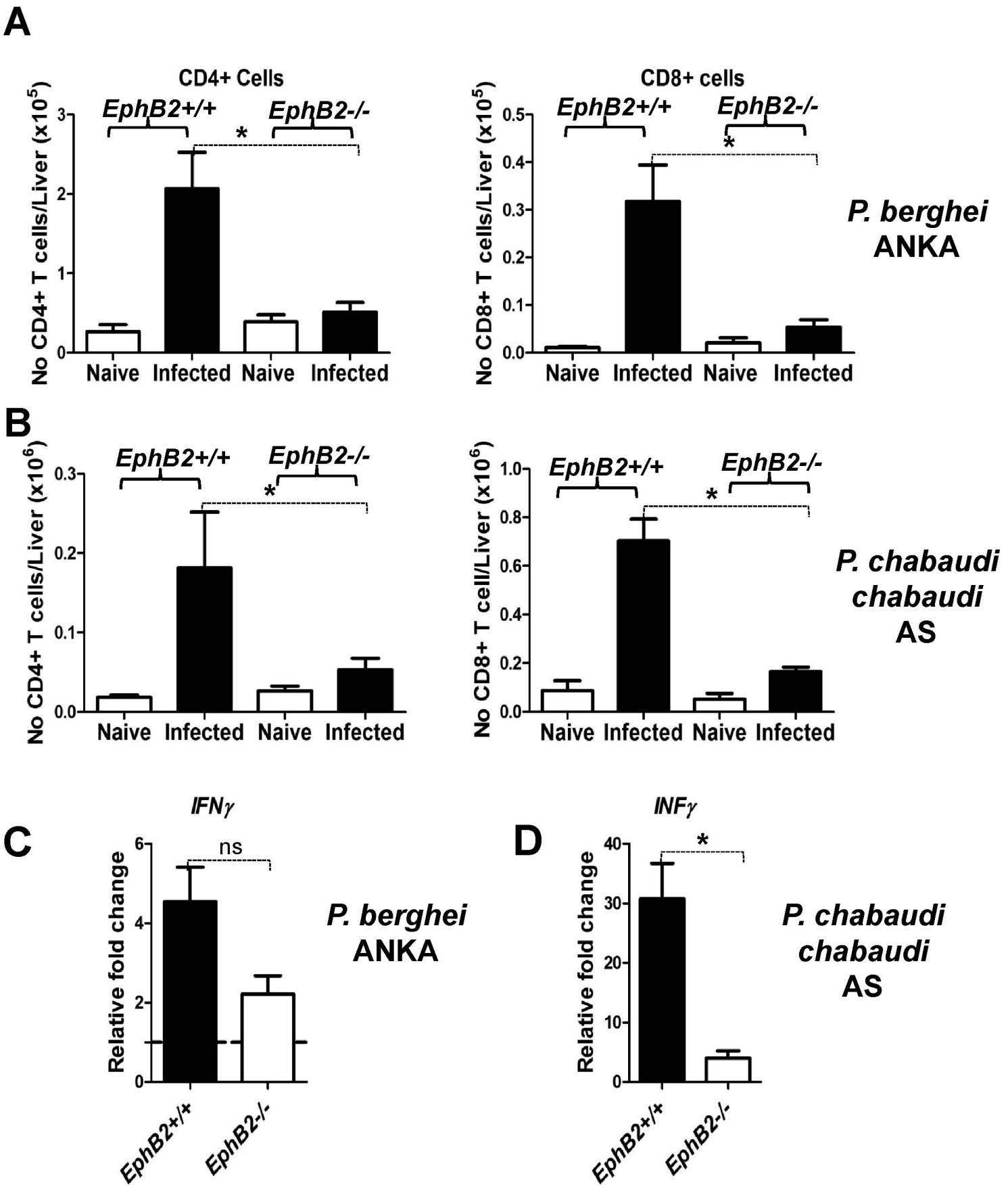

This article is protected by copyright. All rights reserved.

Figure S8:

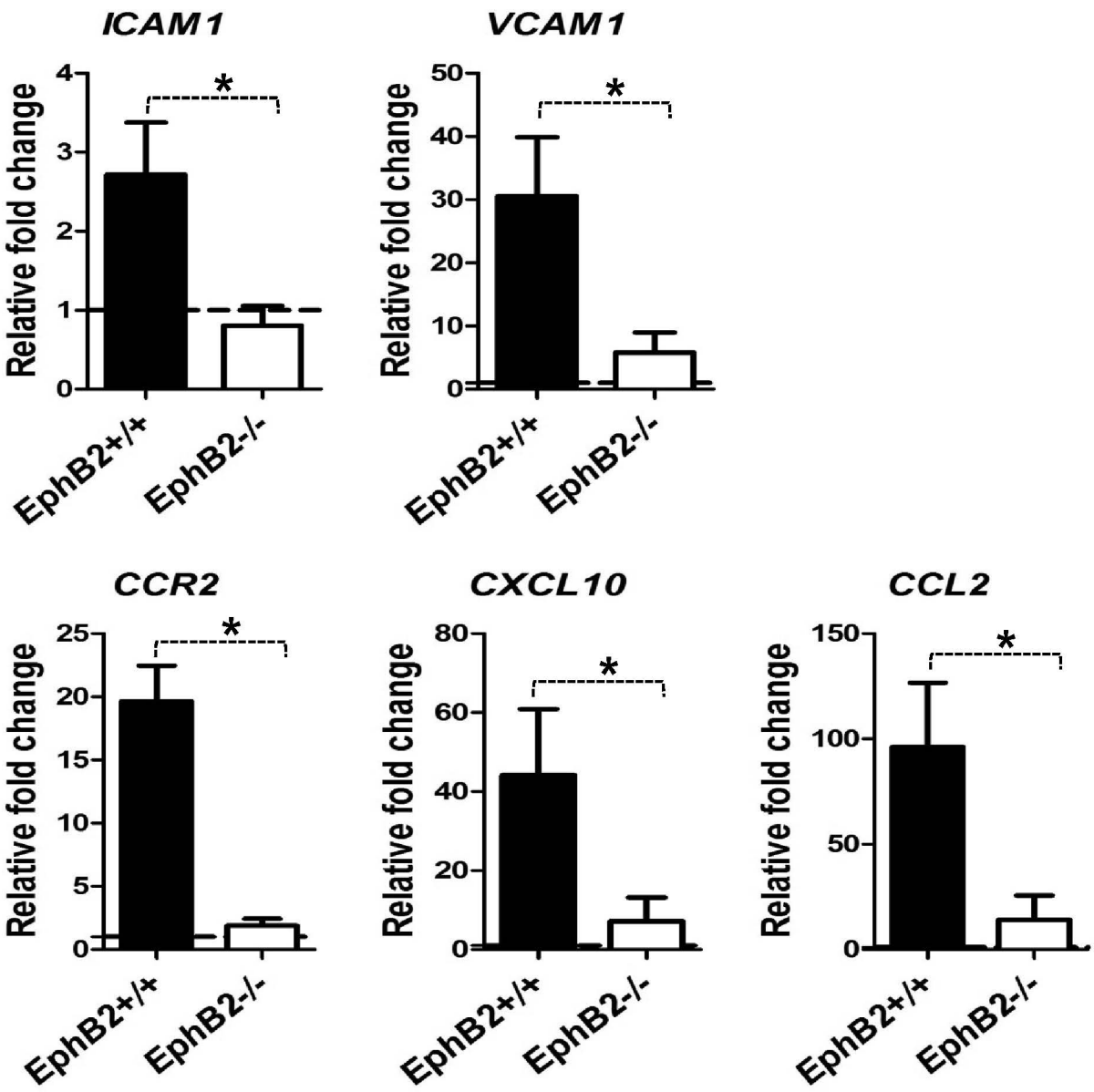

This article is protected by copyright. All rights reserved.

Figure S9:

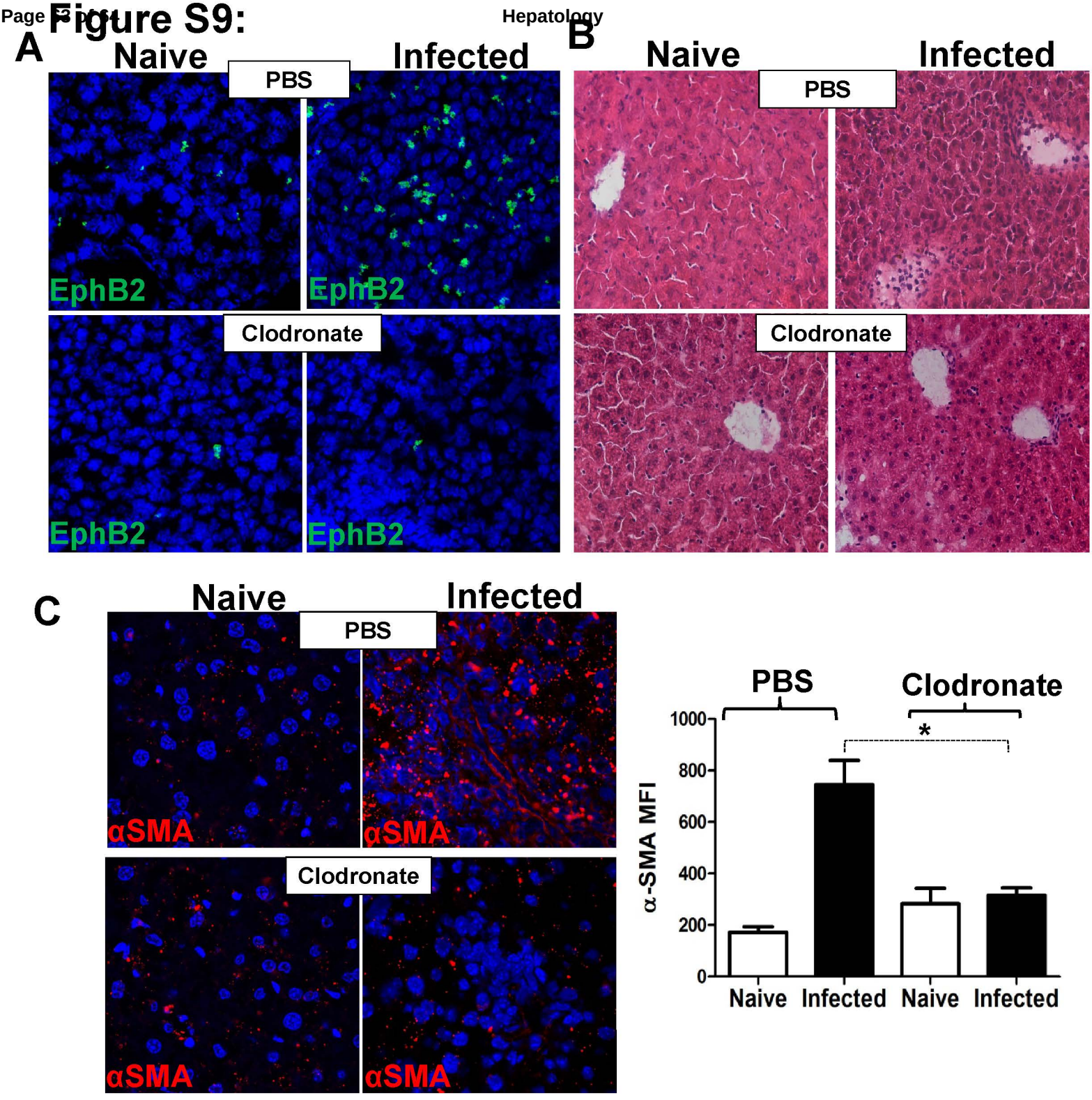

Hepatology
This article is protected by copyright. All rights reserved.

Figure S10

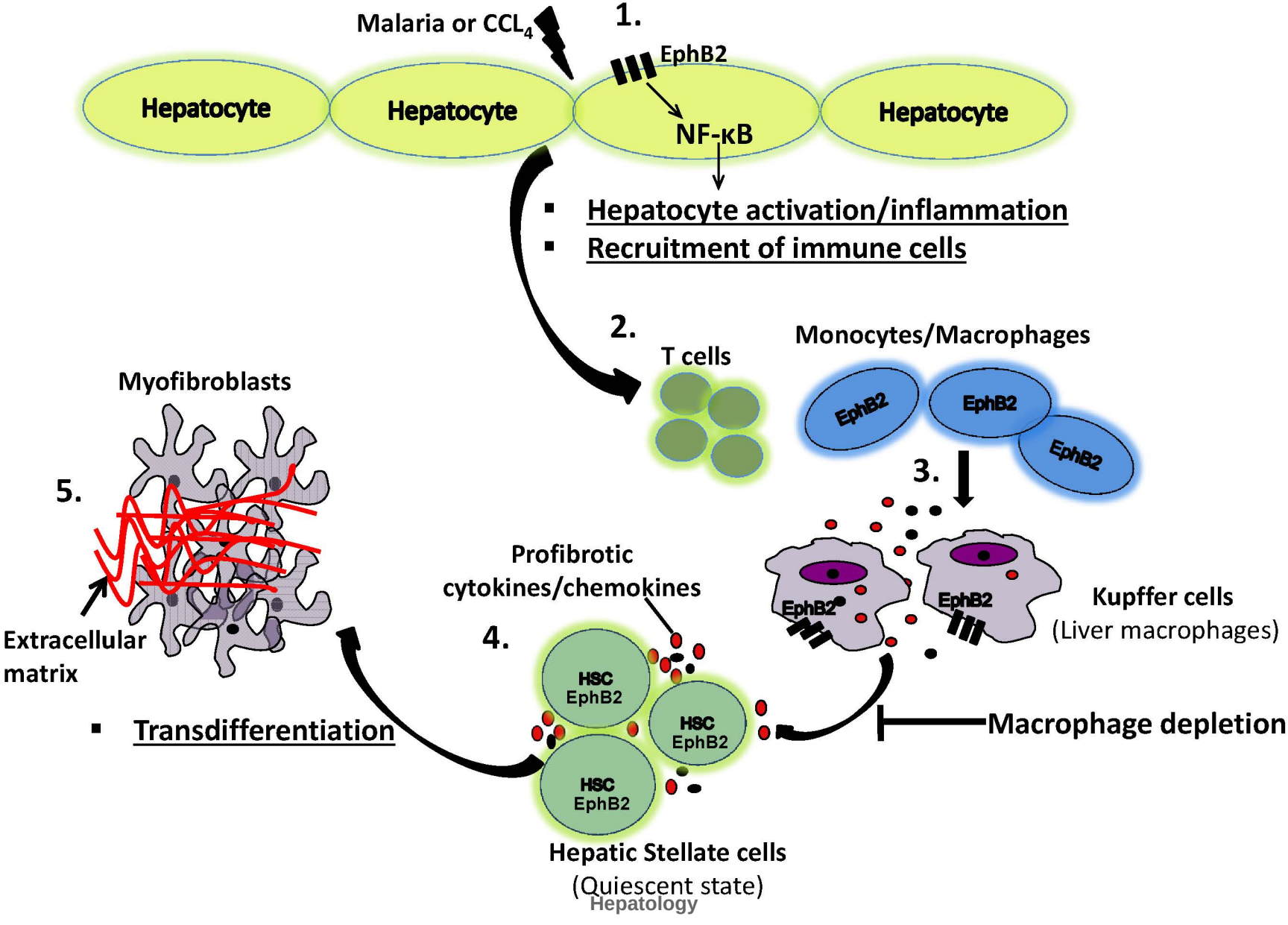

This article is protected by copyright. All rights reserved.